

BABAR: Search for Lepton Flavor Violation in tau decay

Marcello A. Giorgi

(on behalf of the BABAR Collaboration)

INFN & Universita' di Pisa



08/15/2009

Marcello A. Giorgi



Outline

- Theory Overview
- The BaBar Detector

- $\tau \rightarrow \ell \gamma$
- $\tau \rightarrow \ell \ell \ell$
- $\tau \rightarrow \ell V^0$

- Conclusion



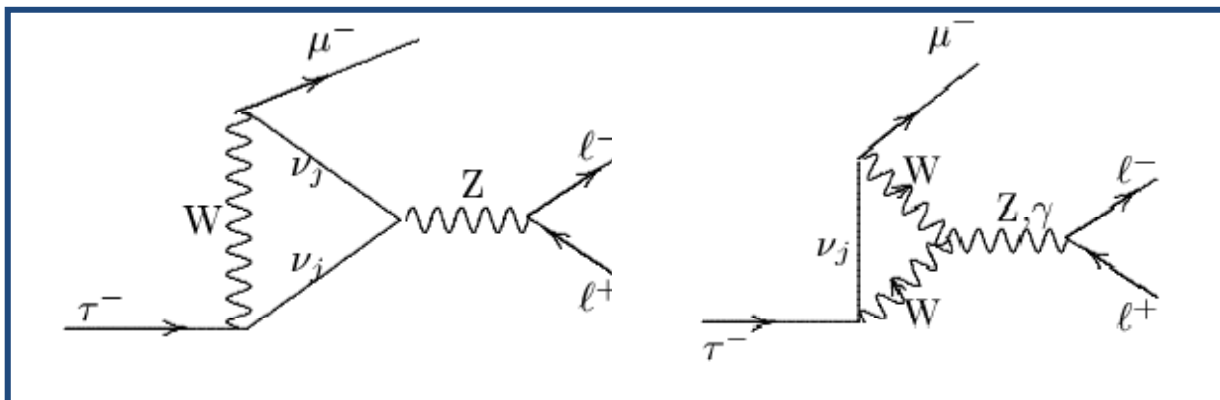
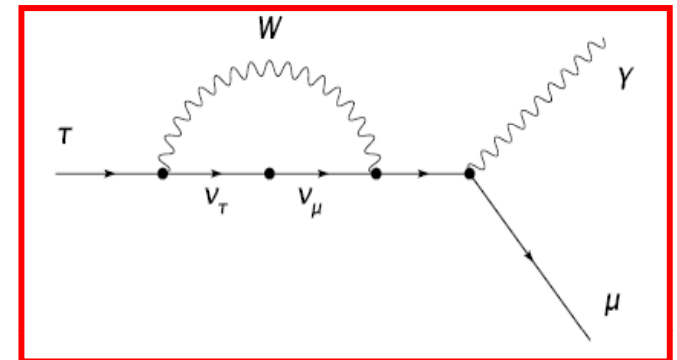
SM prediction for LFV in τ decay

Standard Model allows LFV. Suppressed by (quasi)-degenerate neutrino masses.

In charged leptons it can occur in loops with expected branching fractions well below present sensitivities.

E.g.: expected BF ($\tau \rightarrow \mu \gamma$) $< O(10^{-54})$

Similarly BF ($\tau \rightarrow \ell \ell \ell$) $< O(10^{-54})$

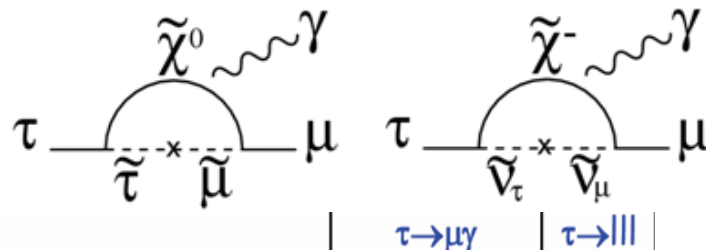


If detected, LFV would imply New Physics with present (and near future) luminosities.

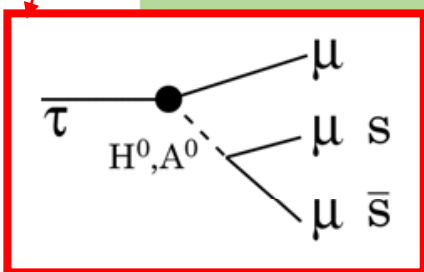
Many New Physics models predict τ LFV BF up to $[O(10^{-8})]$.

Some model predictions

In SUSY LFV decays are generated via slepton mixing



		$\tau \rightarrow \mu \gamma$	$\tau \rightarrow \mu \mu \mu$
SM + ν mixing	Lee, Shrock, PRD 16 (1977) 1444 Cheng, Li, PRD 45 (1980) 1908	Undetectable	
SUSY Higgs	Dedes, Ellis, Raidal, PLB 549 (2002) 159 Brignole, Rossi, PLB 566 (2003) 517	10^{-10}	10^{-7}
SM + heavy Maj ν_R	Cvetič, Dib, Kim, Kim, PRD 66 (2002) 034008	10^{-9}	10^{-10}
Non-universal Z'	Yue, Zhang, Liu, PLB 547 (2002) 252	10^{-9}	10^{-8}
SUSY SO(10)	Masiero, Vempati, Vives, NPB 649 (2003) 189 Fukuyama, Kikuchi, Okada, PRD 68 (2003) 033012	10^{-8}	10^{-10}
	Ellis, Gomez, Leontaris, Lola, Nanopoulos, EPJ C14 (2002) 319 Ellis, Hisano, Raidal, Shimizu, PRD 66 (2002) 115013	10^{-7}	10^{-9}



Looking at NP flavor structure

- Different models expect different processes leading to LFV in charged sector
- If LFV is observed NP flavor structure may be investigated by looking at LFV BF Ratios.

Ratio	SM + Seesaw	LHT	MSSM (no Higgs)	Higgs + MSSM
$\mathcal{B}(\tau \rightarrow \mu\mu\mu)/\mathcal{B}(\tau \rightarrow \mu\gamma)$	0.1	0.4-2.3	$2 \cdot 10^{-3}$	0.06-0.1
$\mathcal{B}(\tau \rightarrow e\mu\mu)/\mathcal{B}(\tau \rightarrow e\gamma)$	~ 0.01	0.3-1.6	$2 \cdot 10^{-3}$	0.02-0.04
$\mathcal{B}(\tau \rightarrow eee)/\mathcal{B}(\tau \rightarrow e\mu\mu)$		1.3-1.7	5	0.3-0.5
$\mathcal{B}(\tau \rightarrow \mu\mu\mu)/\mathcal{B}(\tau \rightarrow \mu ee)$		1.2-1.6	0.2	0.08-0.15
$\mathcal{B}(\tau eee)/\mathcal{B}(\tau \rightarrow e\gamma)$	0.1	0.4-2.3	0.01	0.01
$\mathcal{B}(\tau \rightarrow \mu ee)/\mathcal{B}(\tau \rightarrow \mu\gamma)$	~ 0.01	0.3-1.6	0.01	0.01

[arxiv: [hep-ph/0610344v3](https://arxiv.org/abs/hep-ph/0610344v3) and [hep-ph/0702136](https://arxiv.org/abs/hep-ph/0702136)]



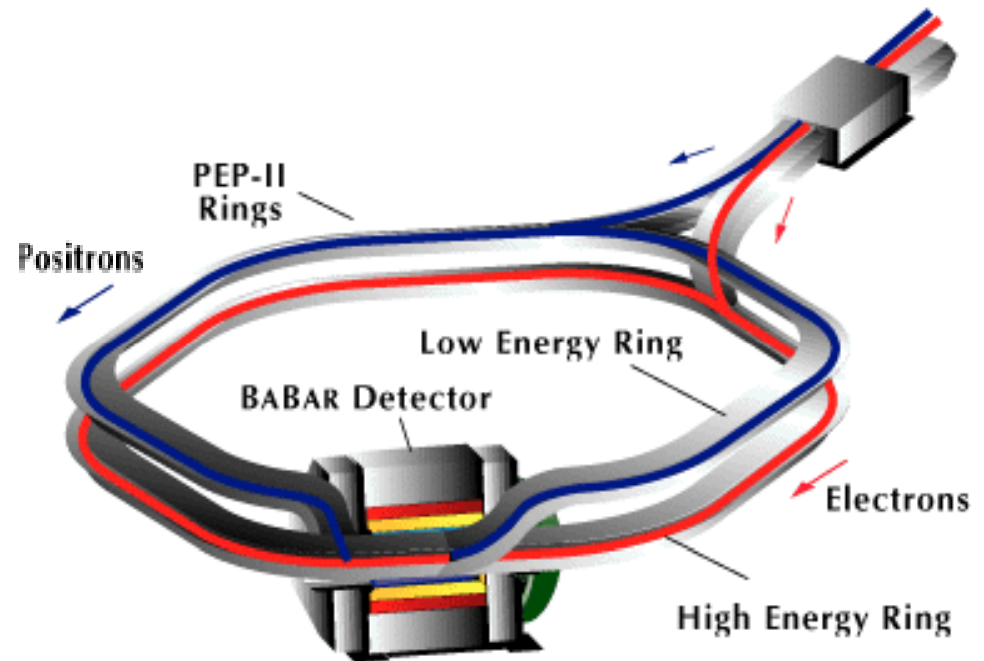
PeP-II and BaBar

Sample Used:

$$\tau \rightarrow \ell \gamma \quad 470 \text{ fb}^{-1} (\Upsilon(4S)) + 31 \text{ fb}^{-1} (\Upsilon(3S)) \\ + 15 \text{ fb}^{-1} (\Upsilon(2S))$$

$$\tau \rightarrow \ell \ell \ell \quad 470 \text{ fb}^{-1} (\Upsilon(4S))$$

$$\tau \rightarrow \ell V^0 \quad 451 \text{ fb}^{-1} (\Upsilon(4S))$$



Signal MC is produced with KK2f + Tauola

Tau decay with Tauola, with the radiation in decay simulated with PHOTOS

Highest peak luminosity 4 times design luminosity : 1.2×10^{34}

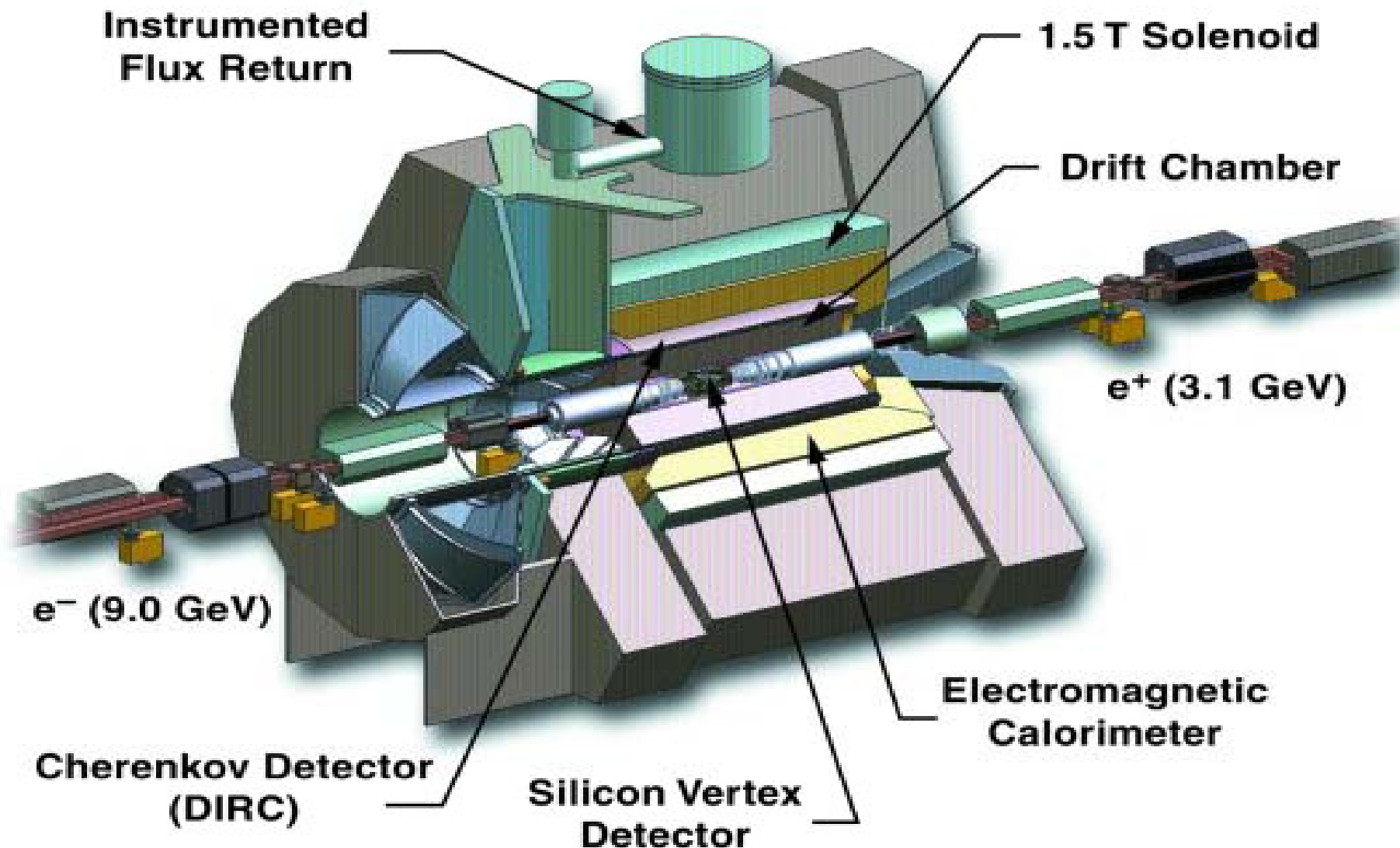
Monthly integrated luminosity 6 times the design : 20 fb^{-1}

Resulting in one of the largest τ data sample

Clean environment for rare process searches



The BaBar Detector



Variables for blind analyses

- All analyses are blind
- Signal and backgrounds scattered in a plane defined by the variables:

$$\Delta E \equiv E_{rec}^* - E_{beam}^*;$$
$$\Delta M_{ec} \equiv M_{rec} - m_\tau = \sqrt{\frac{E_{beam}^{*2}}{c^4} - \frac{|\vec{p}_{3l}^*|^2}{c^2}} - m_\tau$$

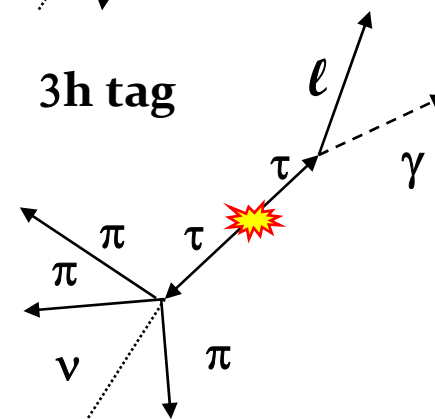
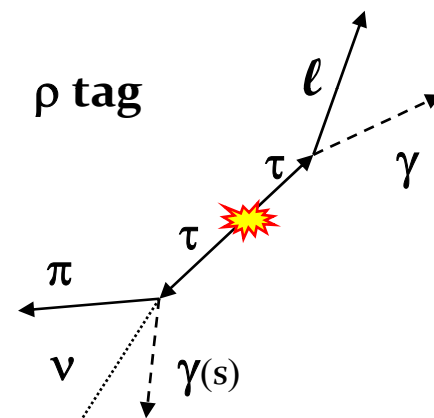
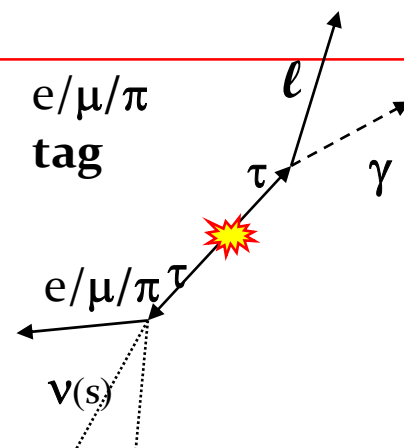
- Resolution is different among channels, worse for channel with electrons:
 - ΔE spread dominated by radiative losses, with larger tails in negative ΔE regions
 - ΔM_{ec} spread dominated by tracking resolution

Search for $\tau \rightarrow \ell \gamma$



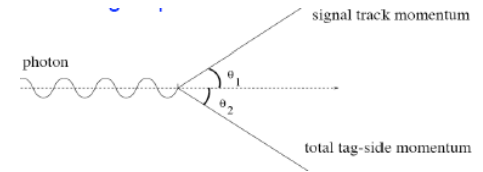
Preselection

- 5 tags considered to minimize backgrounds from QED radiative processes.
- Further Discrimination:
 - Charge conservation
 - Reconstructed mass compatible with τ in tag side
 - $-0.76 < \cos\theta_{\text{miss}} < 0.92$
 - $P_{\text{tag}}/\sqrt{s} < 0.77$ (e/ μ / π), < 0.9 (ρ , 3h)
 - Missing mass > -250 MeV (e/ μ); < 250 MeV (π , 3h) < 500 MeV (ρ)
 - $\text{Cos}\theta_{\text{recoil}} < -0.975$ (e/ μ)



Neural network selector

- NN implemented for each tag.
- Topological info used for radiative QED and $\tau\tau$ backgrounds reduction
- Six variables used as input:
 - Total tag side momentum $[2P_{CM}^{\text{Tag}} / \sqrt{s}]$, Recoil angle $[\text{Cos}\theta_{\text{recoil}}]$, lepton-photon opening angle $[\text{Cos}\theta_{\ell\gamma}]$,
 - Missing Mass $[m_{\nu}^2]$ Missing $p_{T\text{miss}}$ $[-\ln(2 p_{T\text{miss}} / \sqrt{s})]$, ΔE_{γ}

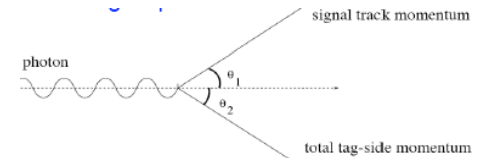
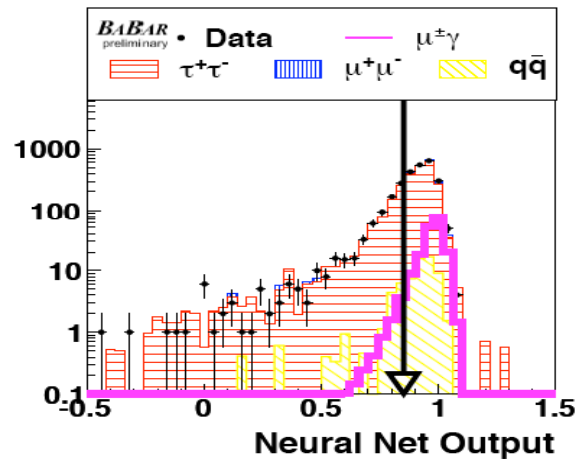
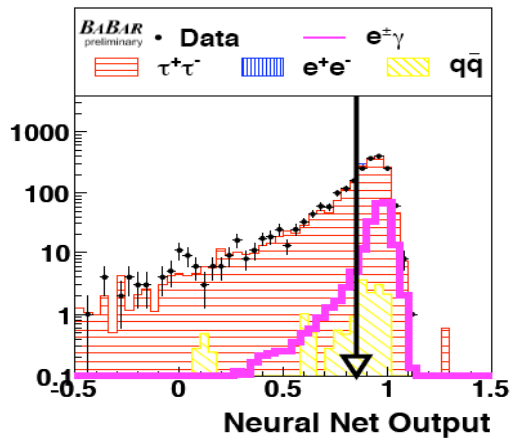


$$\Delta E_{\gamma} \equiv \frac{E_{\gamma}^{CM}}{\sqrt{s}} - \frac{|\sin(\theta_1 + \theta_2)|}{\sin(\theta_1) + \sin(\theta_2) + |\sin(\theta_1 + \theta_2)|}$$



Neural network selector

- NN implemented for each tag.
- Topological info used for radiative QED and $\tau\tau$ backgrounds reduction
- Six variables used as input:
 - Total tag side momentum [$2P_{CM}^{\text{Tag}} / \sqrt{s}$], Recoil angle [$\text{Cos}\theta_{\text{recoil}}$], lepton-photon opening angle [$\text{Cos}\theta_{\ell\gamma}$],
 - Missing Mass [m_{ν}^2] Missing $p_{T\text{miss}}$ [$-\ln(2 p_{T\text{miss}} / \sqrt{s})$], ΔE_{γ}



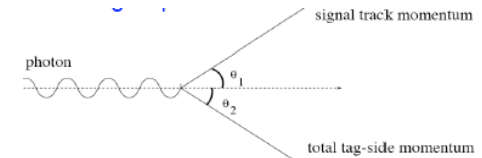
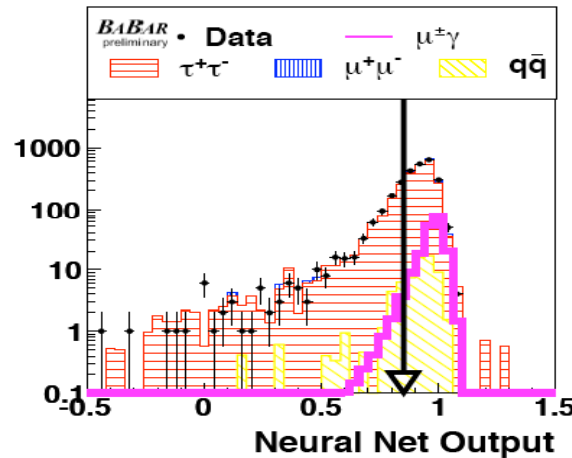
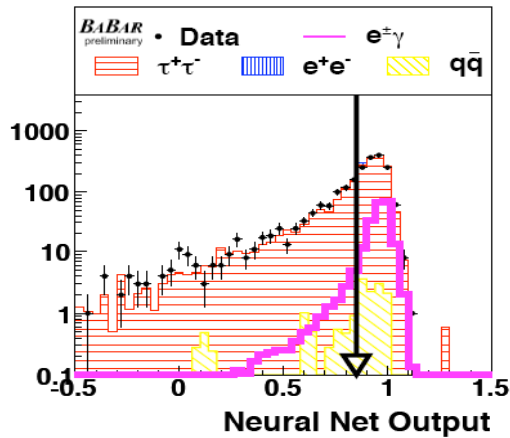
$$\Delta E_{\gamma} \equiv \frac{E_{\gamma}^{CM}}{\sqrt{s}} - \frac{|\sin(\theta_1 + \theta_2)|}{\sin(\theta_1) + \sin(\theta_2) + |\sin(\theta_1 + \theta_2)|}$$

NN Selection
 power is self
 evident from plots.



Neural network selector

- NN implemented for each tag.
- Topological info used for radiative QED and $\tau\tau$ backgrounds reduction
- Six variables used as input:
 - Total tag side momentum [$2P_{\text{Tag}}^{\text{CM}} / \sqrt{s}$], Recoil angle [$\text{Cos}\theta_{\text{recoil}}$], lepton-photon opening angle [$\text{Cos}\theta_{\ell\gamma}$],
 - Missing Mass [m_{ν}^2] Missing p_{Tmiss} [$-\ln(2 p_{\text{Tmiss}} / \sqrt{s})$], ΔE_{γ}



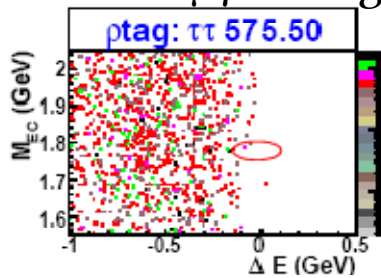
$$\Delta E_{\gamma} \equiv \frac{E_{\gamma}^{CM}}{\sqrt{s}} - \frac{|\sin(\theta_1 + \theta_2)|}{\sin(\theta_1) + \sin(\theta_2) + |\sin(\theta_1 + \theta_2)|}$$

NN Selection power is self evident from plots.

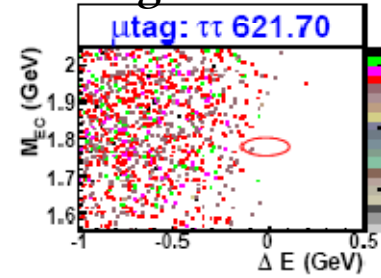
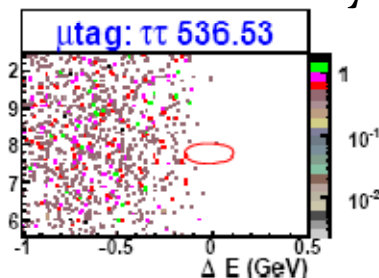
After NN:

For $\tau \rightarrow e\gamma$ backgrounds dominated by τ in μ & ρ tags.

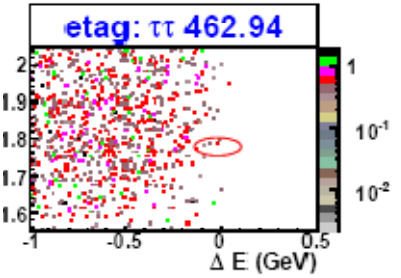
For $\tau \rightarrow \mu\gamma$ backgrounds dominated by τ in μ & e tags



$\tau \rightarrow e\gamma$

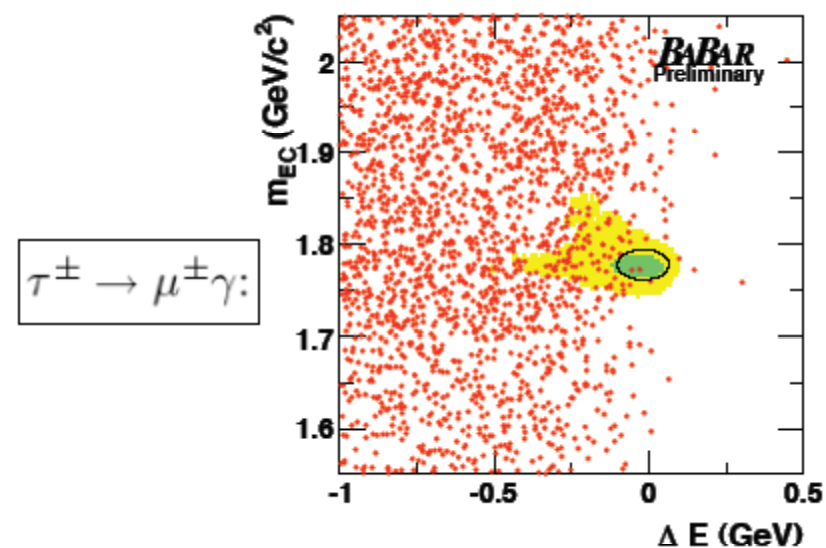
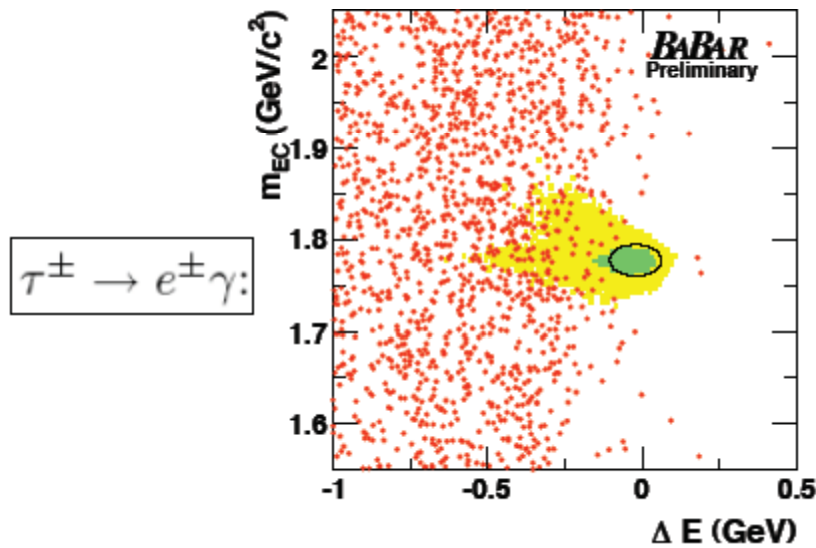


$\tau \rightarrow \mu\gamma$



Results

Data sample used : $\approx (9.676 \pm 7 \times 10^8) \tau$'s, that includes runs @ $Y(3s)$ [3ofb-1] and $Y(2s)$ [15fb-1]



Decay modes	$\langle m_{EC} \rangle$ MeV/c ²	$\sigma(m_{EC})$ MeV/c ²	$\langle \Delta E \rangle$ MeV	$\sigma(\Delta E)$ MeV	2 σ signal ellipse		ϵ (%)	UL ($\times 10^{-8}$)	
					obs.	exp.		obs.	exp.
$\tau^\pm \rightarrow e^\pm \gamma$	1777.3	8.6	-21.4	42.1	0	1.6 ± 0.5	3.91 ± 0.51	3.3	9.8
$\tau^\pm \rightarrow \mu^\pm \gamma$	1777.4	8.3	-18.3	42.2	2	3.6 ± 0.6	6.11 ± 0.50	4.4	8.1

UL measured using Feldman Cousin method.

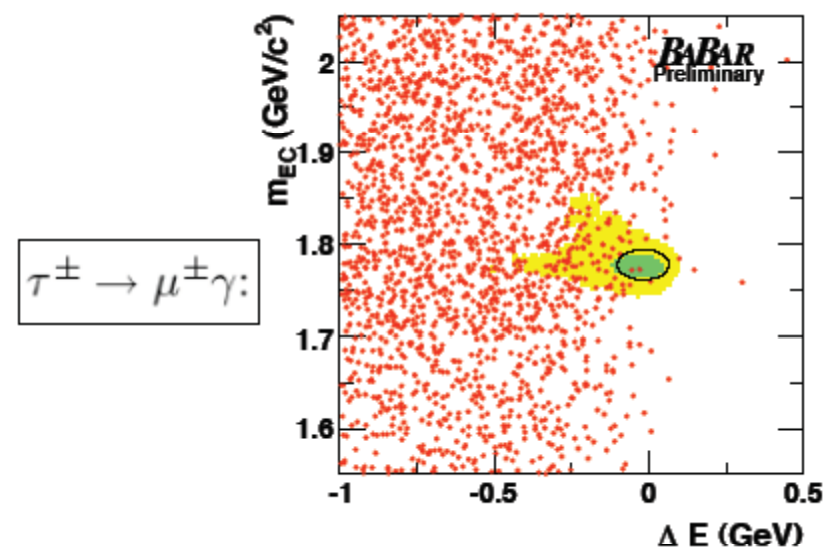
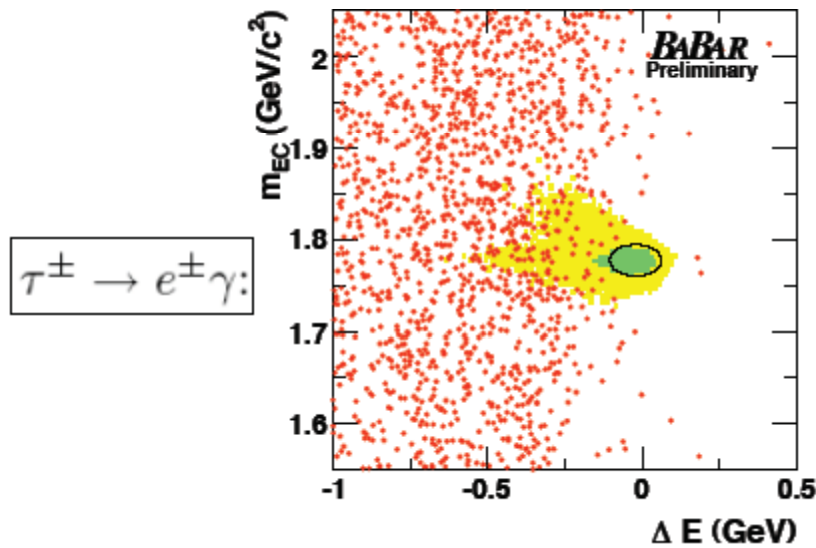
Background estimation validated looking at larger signal

boxes, efficiency estimated from MC studies for each tag and for all tags together

	# of events	-9 σ	-5 σ	+5 σ	+9 σ
$\tau^\pm \rightarrow e^\pm \gamma$	Observed	2	1	2	2
	Expected	1.2 ± 0.2	1.4 ± 0.2	1.9 ± 0.3	2.1 ± 0.3
$\tau^\pm \rightarrow \mu^\pm \gamma$	Observed	3	1	4	6
	Expected	2.8 ± 0.3	3.1 ± 0.3	4.2 ± 0.4	4.8 ± 0.5

Results

Data sample used : $\approx (9.676 \pm 7 \times 10^8) \tau$'s, that includes runs @ $Y(3s)$ [3ofb-1] and $Y(2s)$ [15fb-1]



Decay modes	$\langle m_{EC} \rangle$ MeV/c ²	$\sigma(m_{EC})$ MeV/c ²	$\langle \Delta E \rangle$ MeV	$\sigma(\Delta E)$ MeV	2 σ signal ellipse		ϵ (%)	UL ₁ ($\times 10^{-8}$)	
					obs.	exp.		obs.	exp.
$\tau^\pm \rightarrow e^\pm \gamma$	1777.3	8.6	-21.4	42.1	0	1.6 ± 0.5	3.91 ± 0.51	3.3	9.8
$\tau^\pm \rightarrow \mu^\pm \gamma$	1777.4	8.3	-18.3	42.2	2	3.6 ± 0.6	6.11 ± 0.50	4.4	8.1

No evidence of signal in the 2 σ signal ellipses!

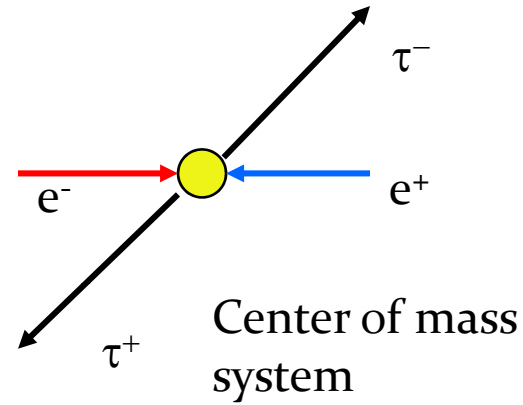
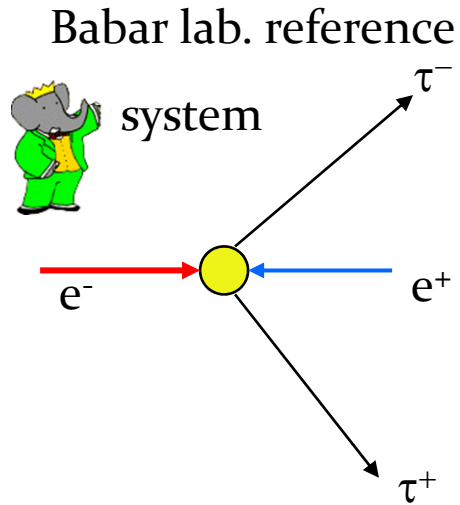
UL measured using Feldman Cousin method.
Background estimation validated looking at larger signal boxes, efficiency estimated from MC studies for each tag and for all tags together

	# of events	-9 σ	-5 σ	+5 σ	+9 σ
$\tau^\pm \rightarrow e^\pm \gamma$	Observed	2	1	2	2
	Expected	1.2 ± 0.2	1.4 ± 0.2	1.9 ± 0.3	2.1 ± 0.3
$\tau^\pm \rightarrow \mu^\pm \gamma$	Observed	3	1	4	6
	Expected	2.8 ± 0.3	3.1 ± 0.3	4.2 ± 0.4	4.8 ± 0.5

Search for $\tau \rightarrow \ell\ell\ell$
Search for $\tau \rightarrow \ell V^0$ (Had Vector Meson)



Pre-selection

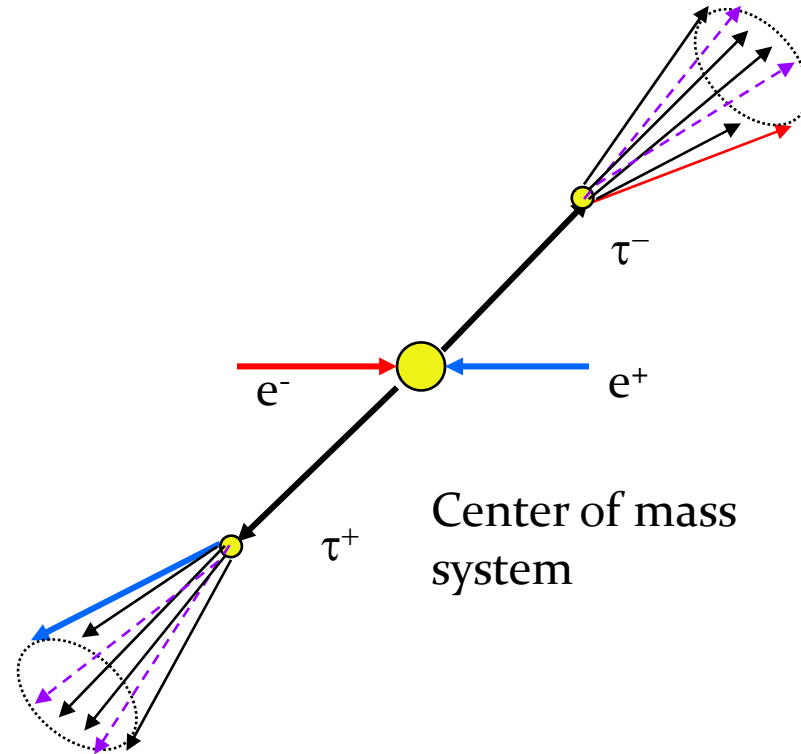
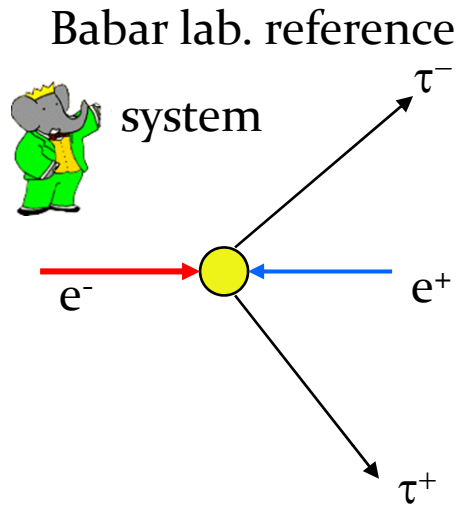


$\tau \rightarrow lll$	$\tau \rightarrow \ell V^0$
$\tau^- \rightarrow e^- e^+ e^-$	$\tau^- \rightarrow \mu^- \rho$
$\tau^- \rightarrow \mu^- e^+ e^-$	$\tau^- \rightarrow e^- \rho$
$\tau^- \rightarrow e^- \mu^+ e^-$	$\tau^- \rightarrow \mu^- K^*$
$\tau^- \rightarrow \mu^- \mu^+ e^-$	$\tau^- \rightarrow e^- \bar{K}^*$
$\tau^- \rightarrow \mu^- e^+ \mu^-$	$\tau^- \rightarrow \mu^- K^*$
$\tau^- \rightarrow \mu^- \mu^+ \mu^-$	$\tau^- \rightarrow e^- K^*$
	$\tau^- \rightarrow \mu^- \Phi$
	$\tau^- \rightarrow e^- \Phi$

In total limits for 14 channels presented



Pre-selection

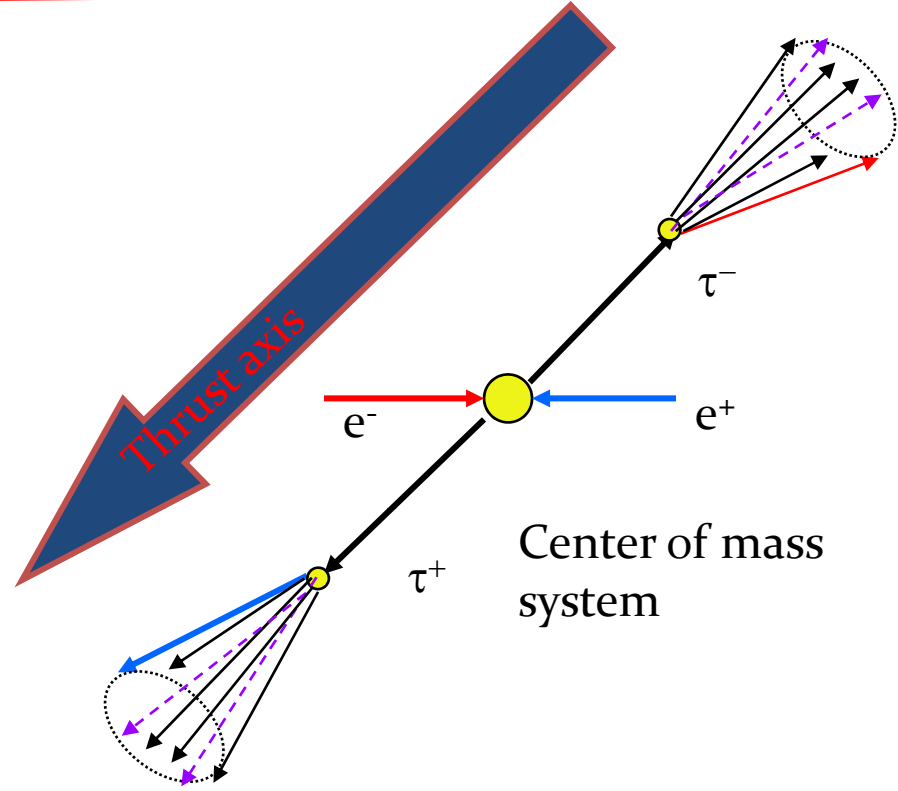
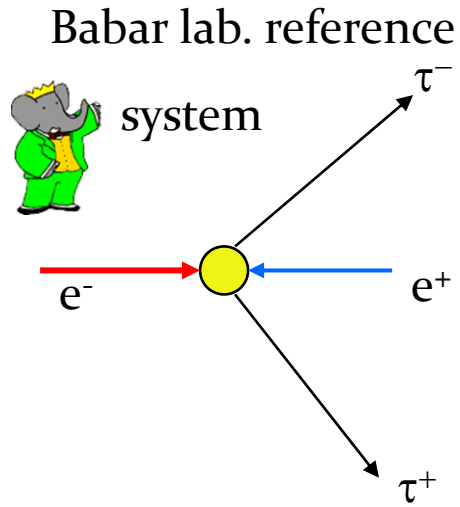


$\tau \rightarrow lll$	$\tau \rightarrow lV^0$
$\tau^- \rightarrow e^-e^+e^-$	$\tau^- \rightarrow \mu^- \rho$
$\tau^- \rightarrow \mu^-e^+e^-$	$\tau^- \rightarrow e^- \rho$
$\tau^- \rightarrow e^- \mu^+e^-$	$\tau^- \rightarrow \mu^- K^*$
$\tau^- \rightarrow \mu^- \mu^+e^-$	$\tau^- \rightarrow e^- \bar{K}^*$
$\tau^- \rightarrow \mu^- e^+ \mu^-$	$\tau^- \rightarrow \mu^- K^*$
$\tau^- \rightarrow \mu^- \mu^+ \mu^-$	$\tau^- \rightarrow e^- K^*$
	$\tau^- \rightarrow \mu^- \Phi$
	$\tau^- \rightarrow e^- \Phi$

In total limits for 14 channels presented



Pre-selection

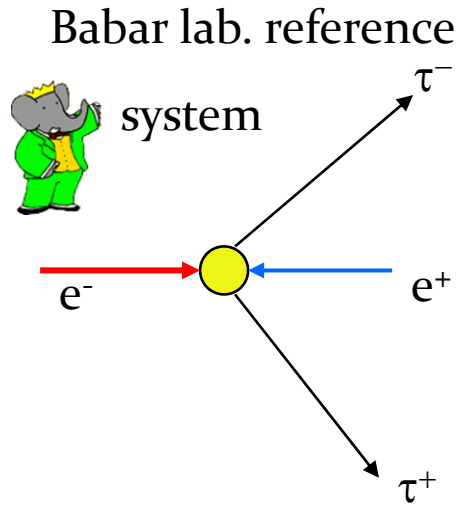


$\tau^- \rightarrow l l l$	$\tau^- \rightarrow l V^0$
$\tau^- \rightarrow e^- e^+ e^-$	$\tau^- \rightarrow \mu^- \rho$
$\tau^- \rightarrow \mu^- e^+ e^-$	$\tau^- \rightarrow e^- \rho$
$\tau^- \rightarrow e^- \mu^+ e^-$	$\tau^- \rightarrow \mu^- K^*$
$\tau^- \rightarrow \mu^- \mu^+ e^-$	$\tau^- \rightarrow e^- \bar{K}^*$
$\tau^- \rightarrow \mu^- e^+ \mu^-$	$\tau^- \rightarrow \mu^- K^*$
$\tau^- \rightarrow \mu^- \mu^+ \mu^-$	$\tau^- \rightarrow e^- K^*$
	$\tau^- \rightarrow \mu^- \Phi$
	$\tau^- \rightarrow e^- \Phi$

In total limits for 14 channels presented

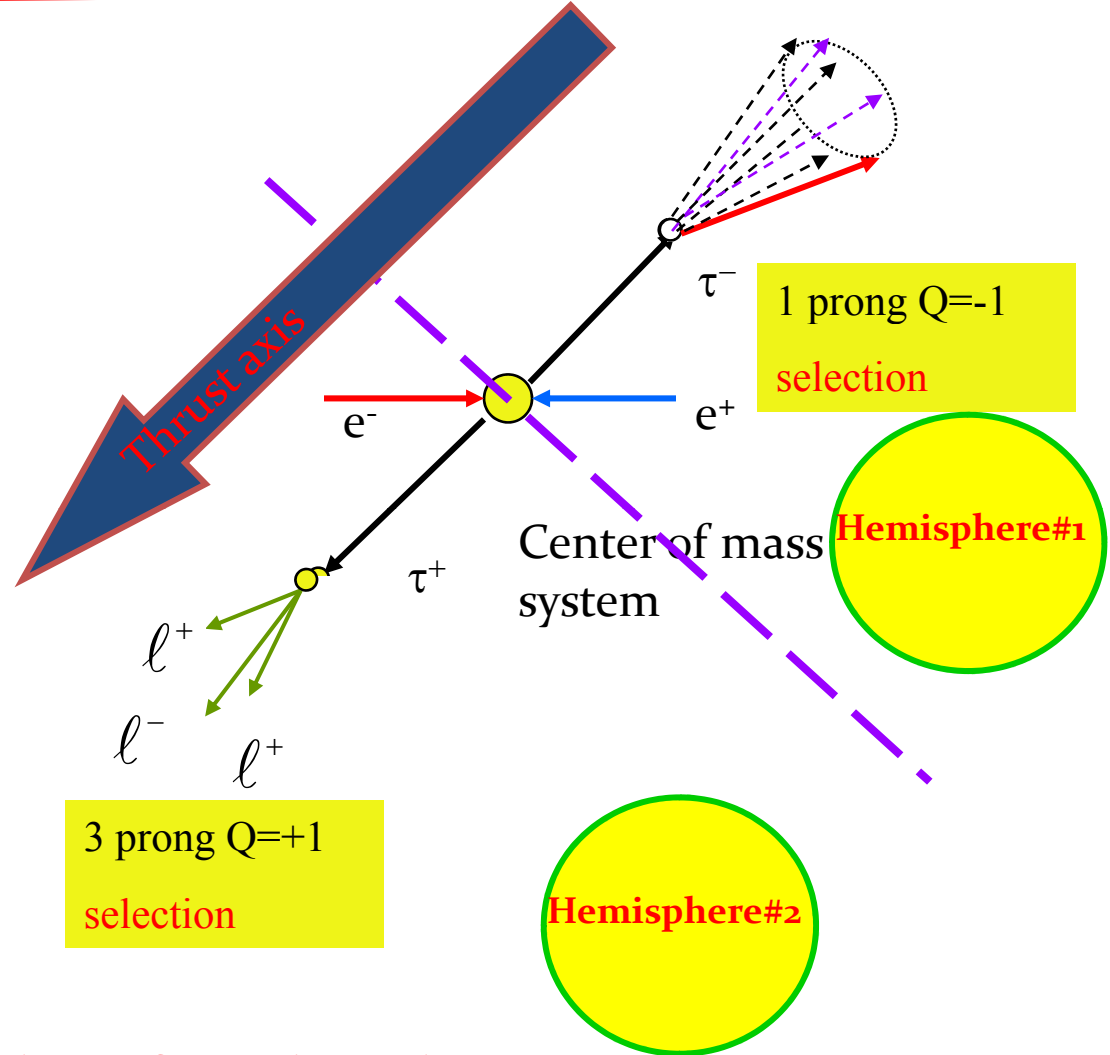


Pre-selection



$\tau^- \rightarrow l l l$	$\tau^- \rightarrow l V^0$
$\tau^- \rightarrow e^- e^+ e^-$	$\tau^- \rightarrow \mu^- \rho$
$\tau^- \rightarrow \mu^- e^+ e^-$	$\tau^- \rightarrow e^- \rho$
$\tau^- \rightarrow e^- \mu^+ e^-$	$\tau^- \rightarrow \mu^- K^*$
$\tau^- \rightarrow \mu^- \mu^+ e^-$	$\tau^- \rightarrow e^- \bar{K}^*$
$\tau^- \rightarrow \mu^- e^+ \mu^-$	$\tau^- \rightarrow \mu^- K^*$
$\tau^- \rightarrow \mu^- \mu^+ \mu^-$	$\tau^- \rightarrow e^- K^*$
	$\tau^- \rightarrow \mu^- \Phi$
	$\tau^- \rightarrow e^- \Phi$

08/15/2009



In total limits for 14 channels presented

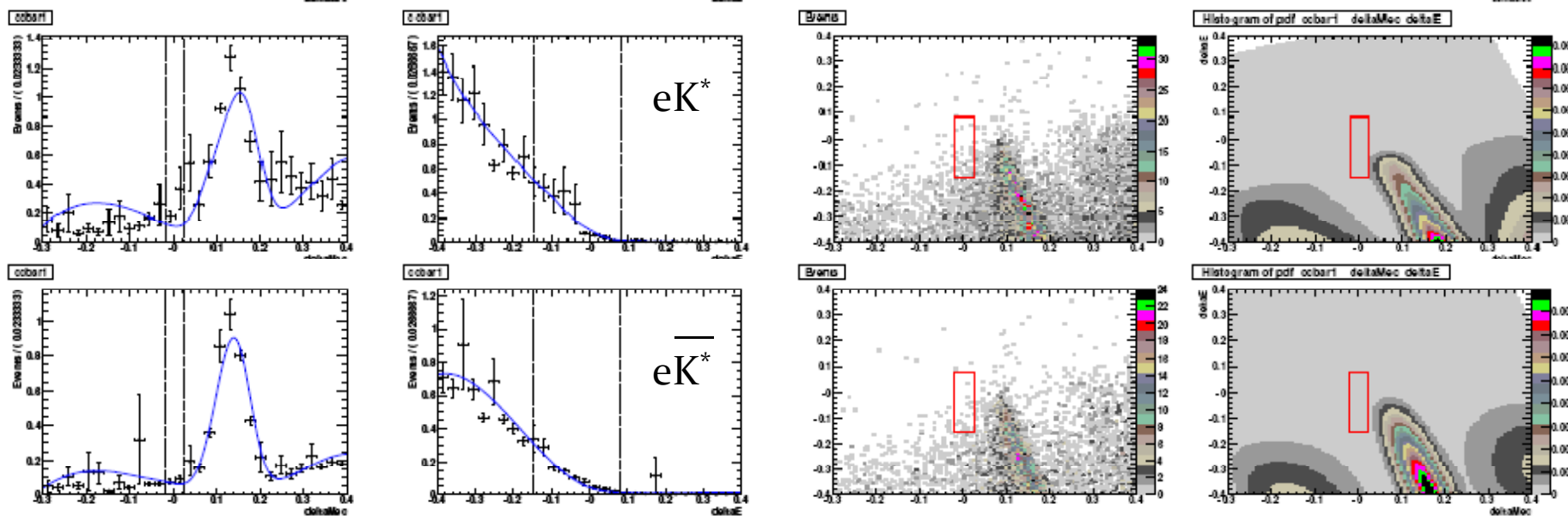
Marcello A. Giorgi



Background Rejection

- 5 main background categories
- We use
 - **Combinatorial** uds background: flat on mass distribution
 - **cc** peaking at D^0 mass, may contain true leptons for $\tau \rightarrow \ell V^0$
 - **QED** radiative events for $\tau \rightarrow \ell \ell \ell$
 - $\tau\tau$ backgrounds with real meson and pions, with neutrinos
 - Irreducible background: $D \rightarrow V^0 \ell \nu$ for $\tau \rightarrow \ell V^0$

Background is parameterized in PDF bi-dimensionally to account for the correlations seen in the plots.



Preliminary

Marcello A. Giorgi

08/15/2009

21



Selection Strategy

Three regions defined in $(\Delta M_{\text{ec}}, \Delta E)$ plane

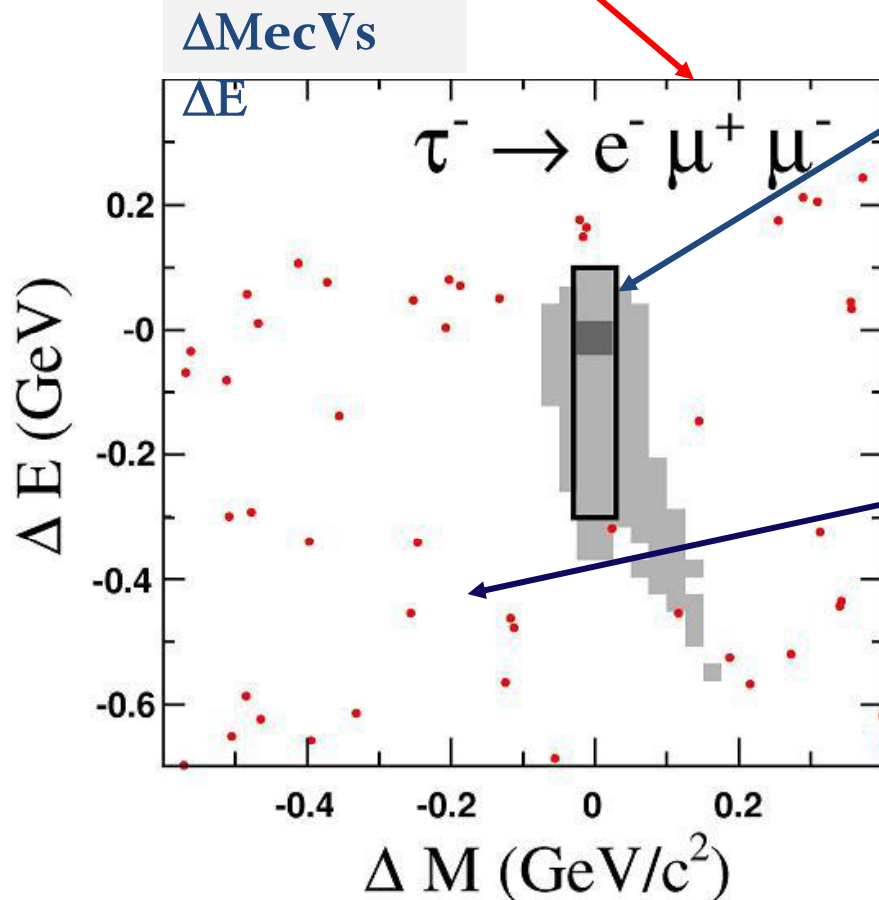
Large Box (LB): identical for all channels. Almost all signal events lie in this region

Signal Box (SB): different for each channel, dimension optimized to give the best UL for each channel.

Data events in this region are **BLIND**

Grand Sideband (GS): is the unblinded region of the LB.

Background estimation made extrapolating data from GS to SB



UL Calculation

UL obtained using Cousins and Highland.

Data sample used : $\approx 8.6 \times 10^8 \tau$'s

Channel	Efficiency (%)	N_{bgd}	Exp. UL	N_{obs}	UL
$e^+e^-e^+$	8.6 ± 0.2	0.12 ± 0.02	3.4×10^{-8}	0	2.9×10^{-8}
$e^+e^-\mu^+$	8.8 ± 0.5	0.64 ± 0.19	3.7×10^{-8}	0	2.2×10^{-8}
$e^+e^+\mu^-$	12.6 ± 0.7	0.34 ± 0.12	2.2×10^{-8}	0	1.8×10^{-8}
$e^+\mu^-\mu^+$	6.4 ± 0.4	0.54 ± 0.14	4.6×10^{-8}	0	3.2×10^{-8}
$e^-\mu^+\mu^+$	10.2 ± 0.6	0.03 ± 0.02	2.8×10^{-8}	0	2.6×10^{-8}
$\mu^+\mu^-\mu^+$	6.6 ± 0.6	0.44 ± 0.17	4.0×10^{-8}	0	3.3×10^{-8}

BABAR	
4.3×10^{-8}	Previous babar: 376fb^{-1} PRL 95:251803, 2007
8.0×10^{-8}	
5.8×10^{-8}	
5.6×10^{-8}	
3.7×10^{-8}	
5.3×10^{-8}	

Major Improvements:

μ eff. 66% \rightarrow 77%

e eff. 89% \rightarrow 91%

Smaller PID syst.

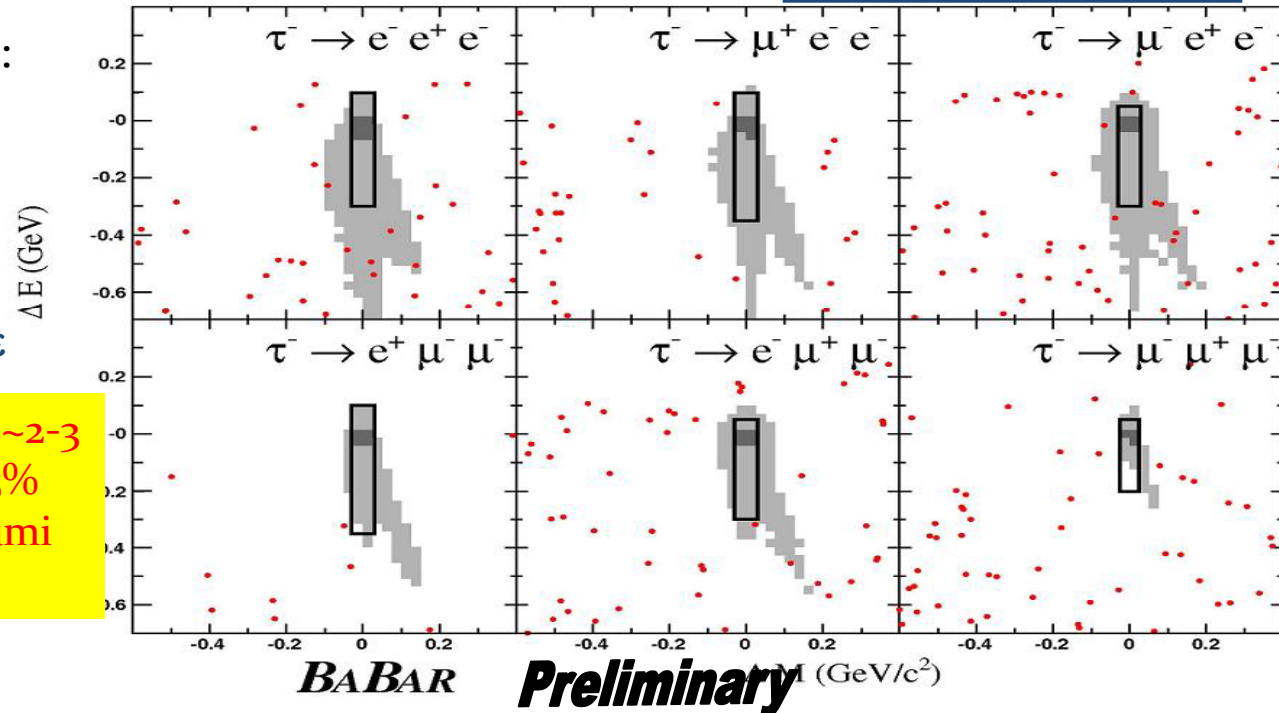
Better selection and ϵ

UL improved by factor $\sim 2-3$

Statistics increase $\sim 25\%$

8 times better than Lumi

Increase only



08/15/2009



UL Calculation

UL obtained using Cousins and Highland.

Data sample used : $\approx 8.6 \times 10^8 \tau$'s

No evidence of signal in the signal box!

Channel	Efficiency (%)	N_{bgd}	Exp. UL	N_{obs}	UL
$e^+e^-e^+$	8.6 ± 0.2	0.12 ± 0.02	3.4×10^{-8}	0	2.9×10^{-8}
$e^+e^-\mu^+$	8.8 ± 0.5	0.64 ± 0.19	3.7×10^{-8}	0	2.2×10^{-8}
$e^+e^+\mu^-$	12.6 ± 0.7	0.34 ± 0.12	2.2×10^{-8}	0	1.8×10^{-8}
$e^+\mu^-\mu^+$	6.4 ± 0.4	0.54 ± 0.14	4.6×10^{-8}	0	3.2×10^{-8}
$e^-\mu^+\mu^+$	10.2 ± 0.6	0.03 ± 0.02	2.8×10^{-8}	0	2.6×10^{-8}
$\mu^+\mu^-\mu^+$	6.6 ± 0.6	0.44 ± 0.17	4.0×10^{-8}	0	3.3×10^{-8}

BABAR	
4.3×10^{-8}	Previous babar: 376fb^{-1} PRL 95:251803, 2007
8.0×10^{-8}	
5.8×10^{-8}	
5.6×10^{-8}	
3.7×10^{-8}	
5.3×10^{-8}	

Major Improvements:

μ eff. 66% \rightarrow 77%

e eff. 89% \rightarrow 91%

Smaller PID syst.

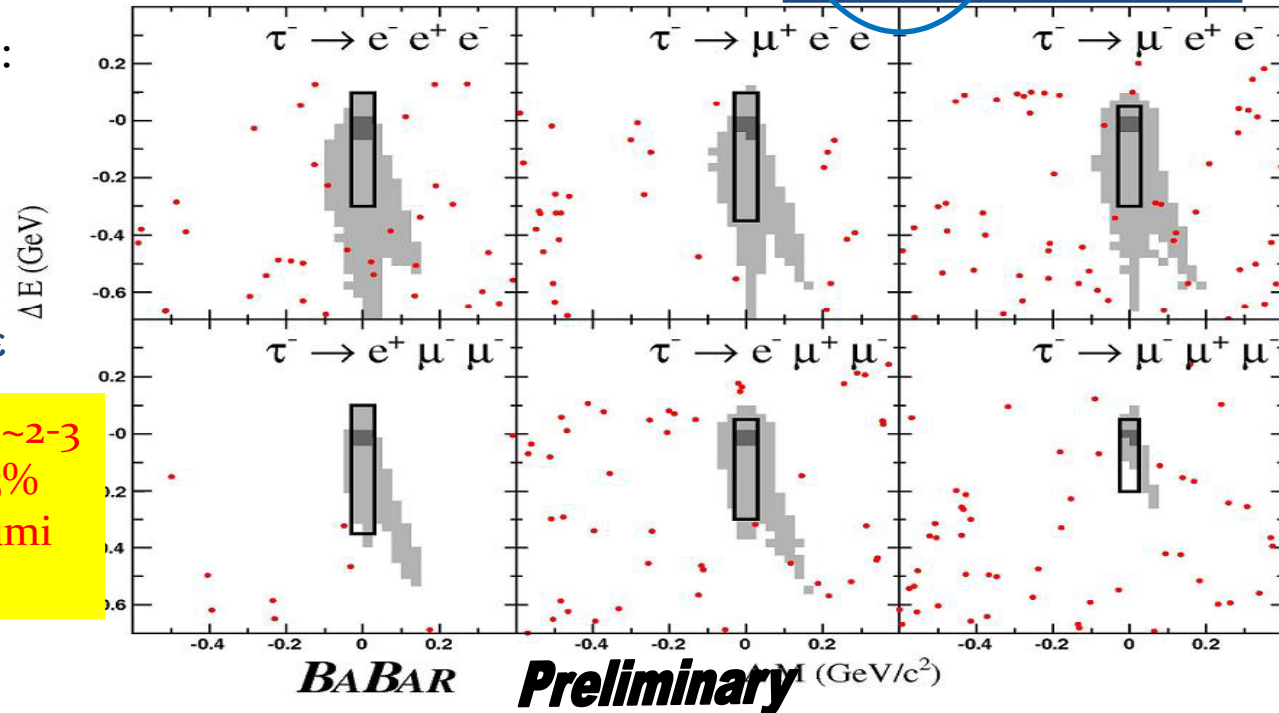
Better selection and ϵ

UL improved by factor $\sim 2-3$

Statistics increase $\sim 25\%$

8 times better than Lumi

Increase only



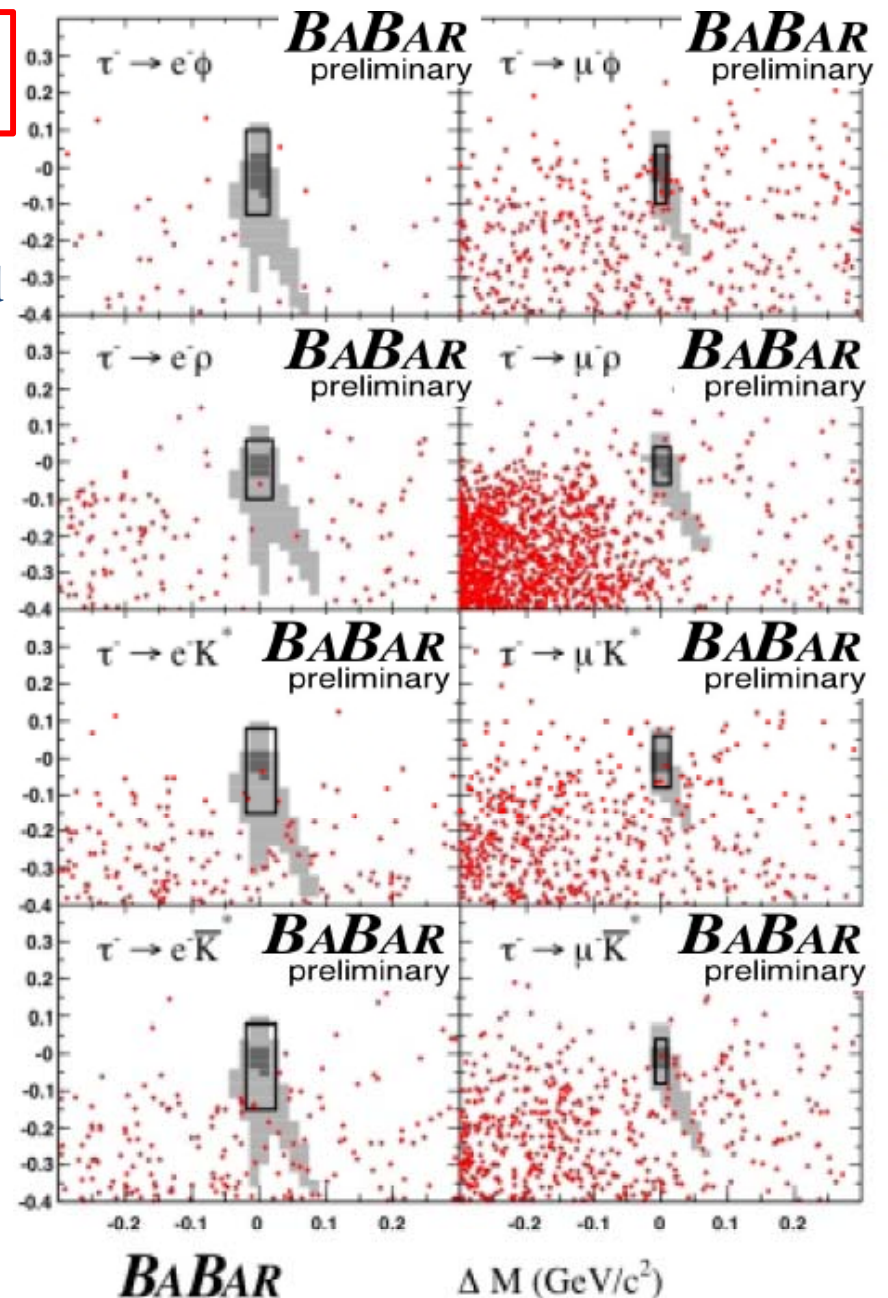
08/15/2009

UL Calculation $\tau \rightarrow \ell V^0$

UL obtained using Cousins and Highland method .

Data sample used : : $\approx 8.3 \times 10^8 \tau$'s

Mode	$\epsilon(\%)$	n_{bkg}	N_{obs}	$UL_{90}(10^{-8})$
$e\rho^0$	7.31 ± 0.18	1.32 ± 0.19	1	4.3
$\mu\rho^0$	4.52 ± 0.41	2.04 ± 0.21	0	0.8
eK^{*0}	8.00 ± 0.18	1.64 ± 0.29	2	5.6
μK^{*0}	4.57 ± 0.36	1.79 ± 0.25	4	16.7
$e\bar{K}^{*0}$	7.76 ± 0.17	2.76 ± 0.30	2	4.0
$\mu\bar{K}^{*0}$	4.11 ± 0.31	1.72 ± 0.18	1	6.4
$e\phi$	6.43 ± 0.18	0.68 ± 0.14	0	3.1
$\mu\phi$	5.18 ± 0.26	2.76 ± 0.21	6	18.2



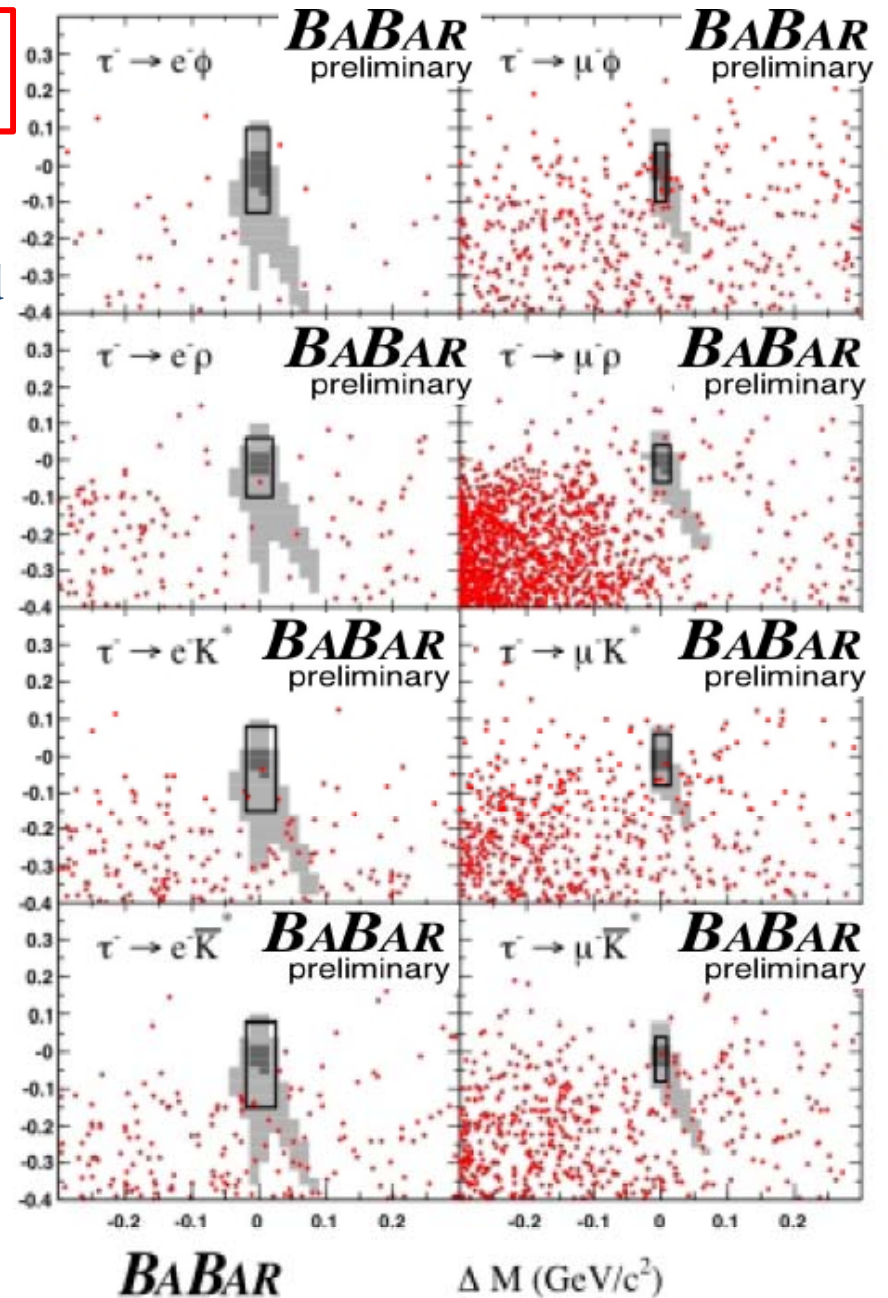
UL Calculation $\tau \rightarrow \ell V^0$

UL obtained using Cousins and Highland method .

Data sample used : : $\approx 8.3 \times 10^8 \tau$'s

No evidence of signal
in the signal box!

Mode	$\epsilon(\%)$	n_{bkg}	N_{obs}	$UL_{90}(10^{-8})$
$e\rho^0$	7.31 ± 0.18	1.32 ± 0.19	1	4.3
$\mu\rho^0$	4.52 ± 0.41	2.04 ± 0.21	0	0.8
eK^{*0}	8.00 ± 0.18	1.64 ± 0.29	2	5.6
μK^{*0}	4.57 ± 0.36	1.79 ± 0.25	4	16.7
$e\bar{K}^{*0}$	7.76 ± 0.17	2.76 ± 0.30	2	4.0
$\mu\bar{K}^{*0}$	4.11 ± 0.31	1.72 ± 0.18	1	6.4
$e\phi$	6.43 ± 0.18	0.68 ± 0.14	0	3.1
$\mu\phi$	5.18 ± 0.26	2.76 ± 0.21	6	18.2



Conclusion

		$\tau \rightarrow \mu \gamma$	$\tau \rightarrow \mu \mu$
SM + ν mixing	Lee, Shrock, PRD 16 (1977) 1444 Cheng, Li, PRD 45 (1980) 1908	Undetectable	
SUSY Higgs	Dedes, Ellis, Raidal, PLB 549 (2002) 159 Brignole, Rossi, PLB 566 (2003) 517	10^{-10}	10^{-7}
SM + heavy Maj ν_R	Cvetič, Dib, Kim, Kim, PRD66 (2002) 034008	10^{-9}	10^{-10}
Non-universal Z'	Yue, Zhang, Liu, PLB 547 (2002) 252	10^{-9}	10^{-8}
SUSY SO(10)	Masiero, Vempati, Vives, NPB 649 (2003) 189 Fukuyama, Kikuchi, Okada, PRD 68 (2003) 033012	10^{-8}	10^{-10}
mSUGRA + Seesaw	Ellis, Gomez, Leontaris, Lola, Nanopoulos, EPJ C14 (2002) 319 Ellis, Hisano, Raidal, Shimizu, PRD 66 (2002) 115013	10^{-7}	10^{-9}

Some predictions are strongly constrained by present results

B-Factories is one of the cleanest environment for LFV searches, great efforts from the BaBar collaboration made it possible to improve measurement more than \sqrt{N} thanks to new tools, that make the analysis more efficient.

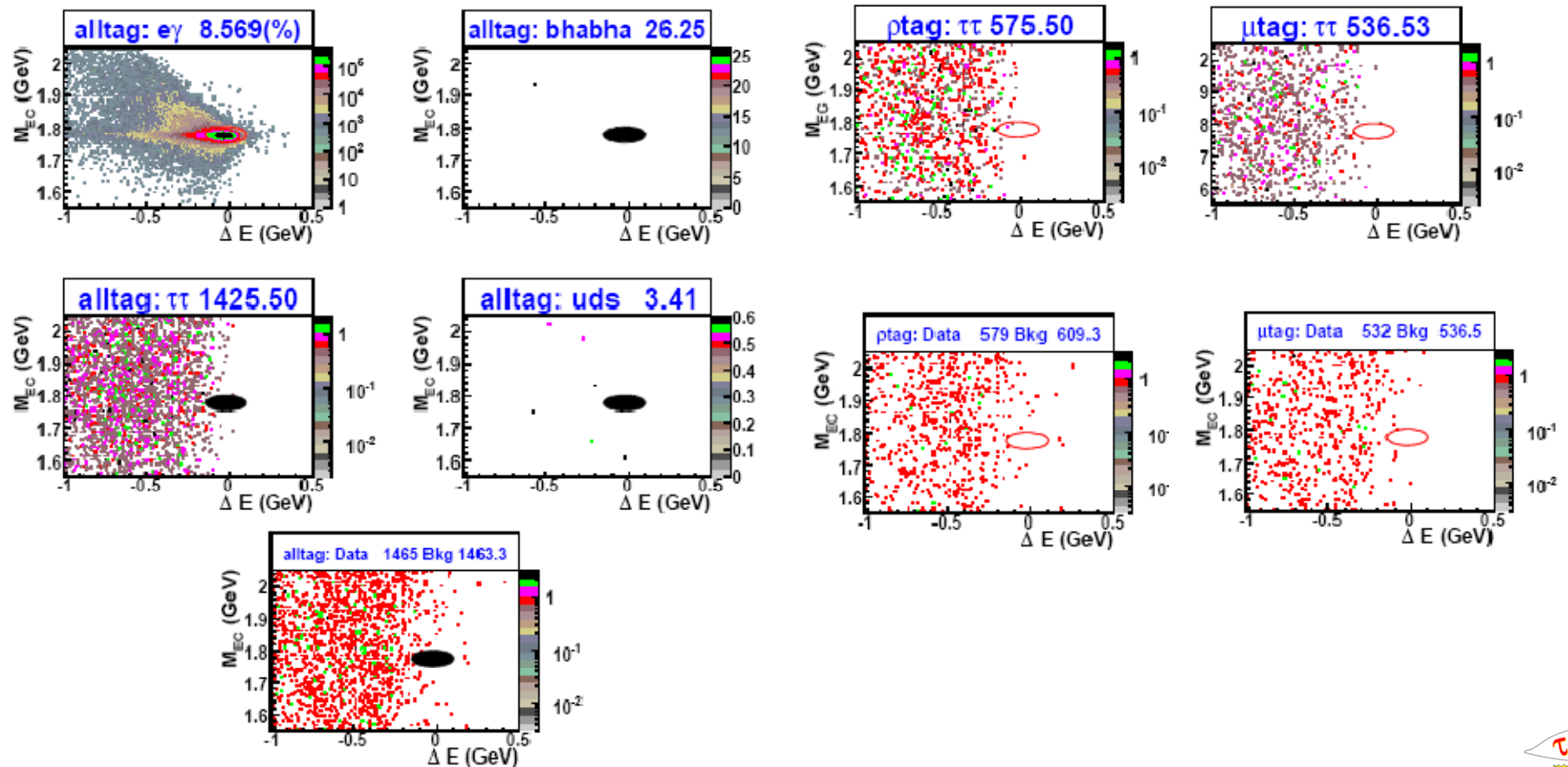


BACKUP



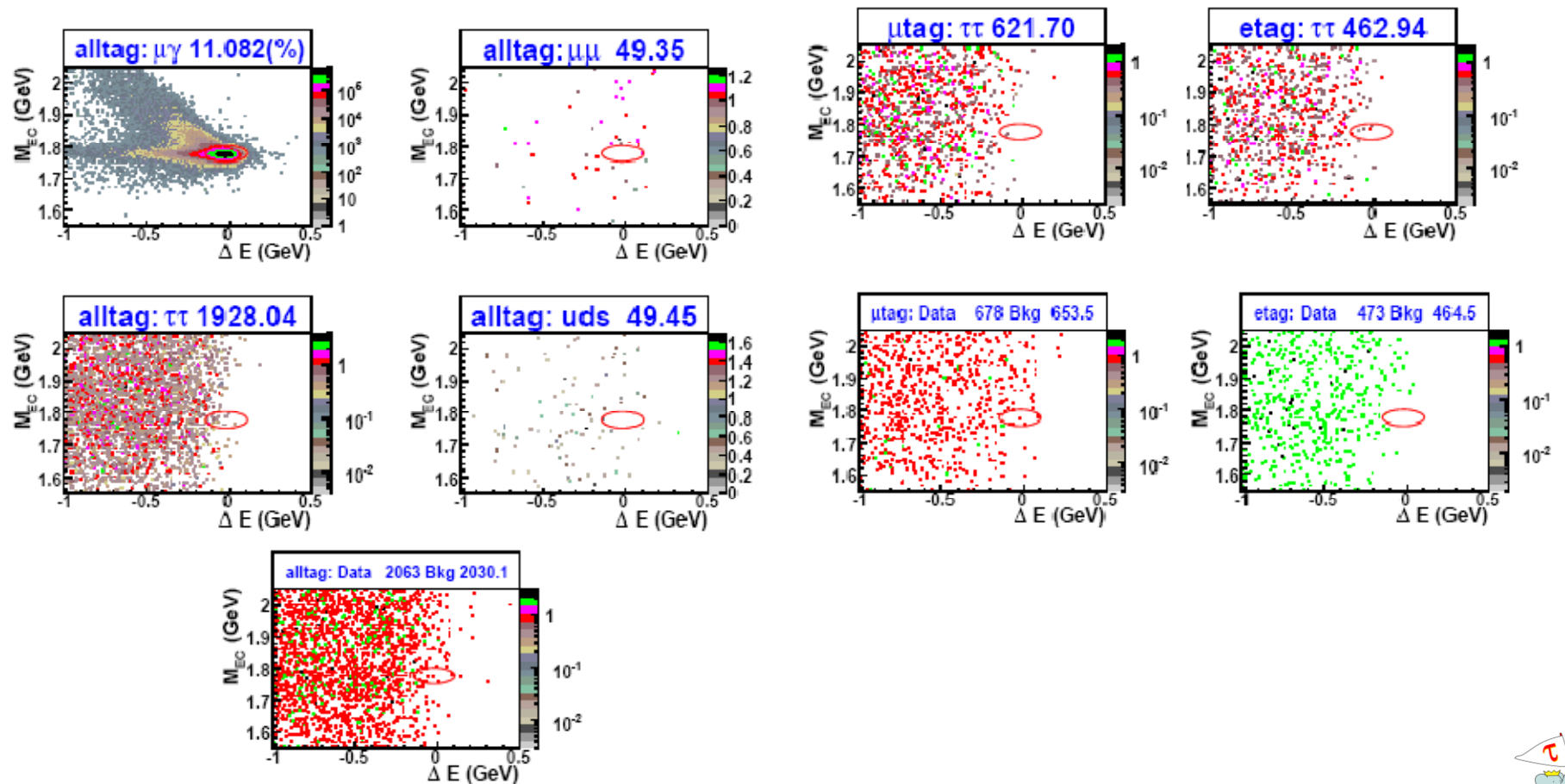
Backgrounds $\tau \rightarrow e\gamma$

- Backgrounds after NN dominated by $\tau\tau$ in μ & ρ tags



Backgrounds $\tau \rightarrow \mu\gamma$

- Backgrounds after NN dominated by τ in μ & e tags



Particle Identification: Event Weighting

- For MC events, PID selection applies a weight rather than rejecting events:
 - Each **MC Track** in signal hemisphere is weighted with a probability, corresponding to the (mis)identification efficiency **in data** for the truth matched particle.
 - For 0.1% of tracks not having MC truth match, average weight is used for tracks.
 - Each **MC Event** is reweighted by the product of the three tracks weights
 - This is a much more efficient use of MC Statistics



Bidimensional Bkg Estimation

Hadronic (uds) backgrounds estimated using a two-dimensional ($\Delta M, \Delta E$) PDF as product of two one-dimensional (P_{Mh}, P_{Eh}) PDF. To avoid correlations a choice of rotated variables is made (empirical parametrization):

$$\Delta M' = \cos(\alpha) \Delta M + \sin(\alpha) \Delta E \quad \Delta E' = -\sin(\alpha) \Delta M + \cos(\alpha) \Delta E$$

$P_{M'}$ is a bifurcated Gaussian. $\Delta E'_0$ [and $\sigma(\Delta E')$], α are free parameters.

Tau backgrounds are estimated with a similar likelihood fit but with same parameterization, but now 2 parameters: α and β .

($e^-e^+e^-$) and ($e^-\mu^+\mu^-$) have large QED background contributions the estimation is done by using a Reverse PID approach.

$c\bar{c}$ backgrounds for $\tau \rightarrow \ell V^0$ channels are divided into subsamples depending on the number of mis-id particles, and fitted with the shape best fitting the category among those used for other categories

Control sample is built with events in the great sideband (LB) passing selections, but PID in 1 prong side.

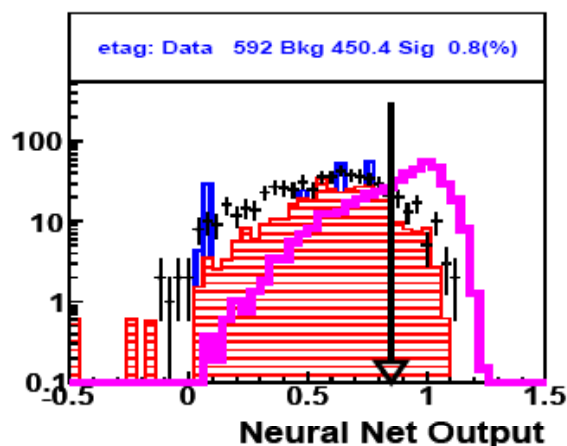
P_{QED} is defined as product of two one dimensional PDF on rotated variables $P_{M'}$ and $P_{E'}$.

$P_{M'}$ is a third order polynomial while $P_{E'}$ is a crystal ball function. A single rotation angle α is used.

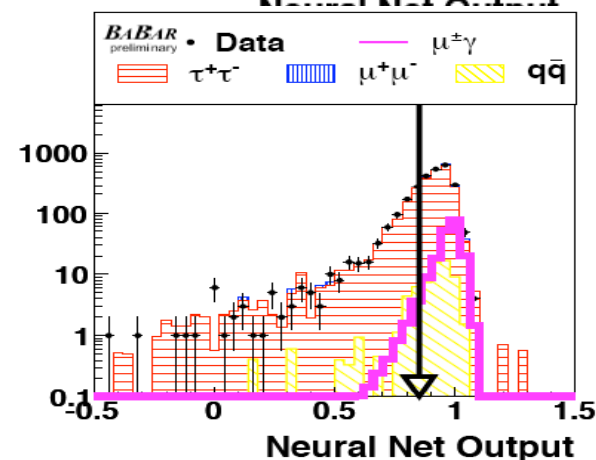
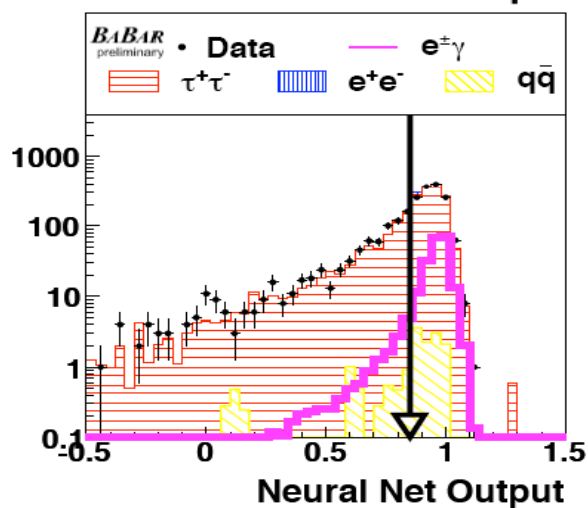
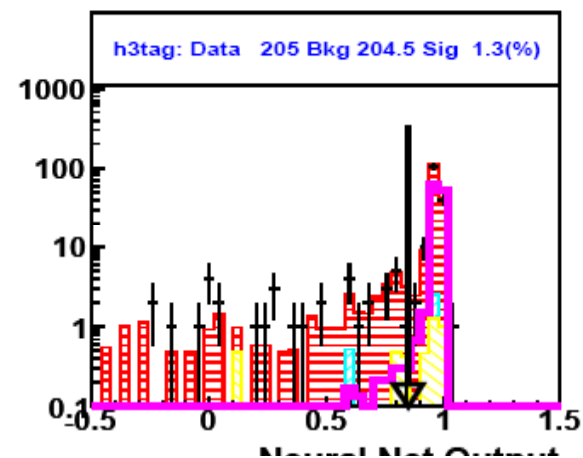
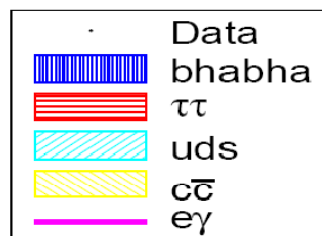


Neural network selector

- NN implemented for each tag.
- Topological info used for radiative QED and τ backgrounds reduction
- Six variables used as input:
 - Total tag side momentum, $\text{Cos}\theta_{\text{recoil}}$, lepton-photon opening angle $\text{Cos}\theta_{\ell\gamma}$,
 - missing ν ., ΔE ..



$$\Delta E_{\gamma} \equiv \frac{E_{\gamma}^{CM}}{\sqrt{s}} - \frac{|\sin(\theta_1 + \theta_2)|}{\sin(\theta_1) + \sin(\theta_2) + |\sin(\theta_1 + \theta_2)|}$$



08/15/2009

Marcello A. Giorgi

33

